

Priority-Aware Shapley Value

Kiljae Lee¹ Ziqi Liu² Weijing Tang² Yuan Zhang¹

Abstract

Shapley values are widely used for model-agnostic data valuation and feature attribution, yet they implicitly assume contributors are interchangeable. This can be problematic when contributors are dependent (e.g., reused/augmented data or causal feature orderings) or when contributions should be adjusted by factors such as trust or risk. We propose **Priority-Aware Shapley Value (PASV)**, which incorporates both hard precedence constraints and soft, contributor-specific priority weights. PASV is applicable to general precedence structures, recovers precedence-only and weight-only Shapley variants as special cases, and is uniquely characterized by natural axioms. We develop an efficient adjacent-swap Metropolis–Hastings sampler for scalable Monte Carlo estimation and analyze limiting regimes induced by extreme priority weights. Experiments on data valuation (MNIST/CIFAR10) and feature attribution (Census Income) demonstrate more structure-faithful allocations and a practical sensitivity analysis via our proposed “priority sweeping”.

1. Introduction

Recent advances in machine learning have fueled growing interest in *data-centric AI* and *explainable AI*, where a central goal is to quantify how much each training example (data valuation) or each input variable (feature attribution) contributes to a model’s performance or predictions (Zha et al., 2025; Mersha et al., 2024). Shapley-type values are a standard tool for *model-agnostic* attribution (Shapley, 1953; Ghorbani & Zou, 2019; Lundberg & Lee, 2017; Kwon & Zou, 2021; Wang & Jia, 2023). A key axiomatization choice behind the classical Shapley value is that it averages marginal contributions over *all* player permutations, implicitly treating players as interchangeable.

¹Department of Statistics, The Ohio State University, OH, USA ²Department of Statistics and Data Science, Carnegie Mellon University, PA, USA. Correspondence to: Yuan Zhang <yzhanghf@stat.osu.edu>.

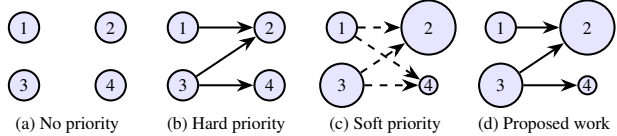


Figure 1. Illustration of priority structures. Dashed arrows in (c): existing works on (c) require special precedence structures.

However, in many modern machine learning applications, this exchangeability is questionable for two distinct reasons. First, players can exhibit *precedence relations* in between. For example, training data may be augmented, copied, or otherwise reused, so a downstream contribution can be largely derivative of an upstream source (Aas et al., 2021); likewise, domain or causal knowledge can impose that some features precede others, making certain orders scientifically meaningless (Frye et al., 2021; Janzing et al., 2020). Recent work further highlights that Shapley-type payoff methods can face *copier attack*. This has inspired replication-robust formulations (Han et al., 2022; Falconer et al., 2025) and group-based approaches (Lee et al., 2025) designed to mitigate such manipulations, reinforcing the need to explicitly incorporate precedence into valuation.

Second, practitioners often have *trust/risk considerations*, e.g., some data points may be less trusted for their independence, more costly to curate, or carry higher legal/compliance risk (Wu et al., 2023; Wang & Jia, 2023). Therefore, attribution should reflect two types of *priority*: (i) *hard priority* that rules out orders violating known precedence, and (ii) *soft priority* that adjusts the attribution computation between players under the hard priority infrastructure.

Existing Shapley variants typically address these two aspects in isolation. Precedence-based methods restrict attention to precedence-feasible orders (Faigle & Kern, 1992), while weight-based methods bias the ordering distribution via player-specific weights, but exclusively for special precedence structures (Kalai & Samet, 1987; Nowak & Radzik, 1995). Recent machine learning adaptations apply these ideas to data valuation and feature attribution (Zheng et al., 2025; Frye et al., 2020), but commonly rely on coarse precedence specifications that are easy to handle computationally without offering a unified mechanism to combine *general* precedence constraints with *individual* priorities.

To this end, we propose the **Priority-Aware Shapley Value**

(PASV), a single Shapley-type attribution method that simultaneously captures (i) *hard* precedence constraints among players, and (ii) *soft* player-specific priority weights (Figure 1). PASV computes each player’s value by averaging its marginal contribution over precedence-feasible orders, while biasing the order distribution according to the specified priorities. This unified view is designed to be both expressive (supporting general precedence constraints) and practically feasible (supporting scalable computation for large player sets).

Our main contributions are:

- **Unified formulation.** We introduce PASV, a Shapley-type value that simultaneously incorporates general precedence constraints and soft priority weights within one coherent random-order framework.
- **Theory and interpretability.** We provide an axiomatic characterization that singles out PASV as a canonical precedence-respecting, weight-aware rule, and we analyze limiting regimes that clarify how extreme priorities can modify the underlying precedence structure.
- **Scalable computation.** We develop an efficient MCMC-based estimator for sampling precedence-feasible orders under non-uniform weighting, enabling Monte Carlo estimation under general precedence.
- **Practical diagnostic via priority sweeping.** Beyond producing a single allocation, PASV provides an actionable *priority-sweeping* stress test: by varying one player (or group)’s weight while keeping others’ weights and the precedence graph fixed, practitioners can quantify the sensitivity to trust/risk considerations, flag contributors whose credit is unstable and may significantly impact the result, and support more robust valuation/attribution decisions.

2. Preliminaries

2.1. From Shapley Value to Random Order Values

Let $[n] = \{1, \dots, n\}$ denote the set of players (data points, features). For each subset $S \subseteq [n]$, let $U(S)$ be the reward earned by the joint work of members in S : here $U : 2^{[n]} \rightarrow \mathbb{R}$ is called *utility function*. The classical royalty sharing problem asks for a principled method to split the total revenue $U([n])$ to each player, considering their contributions on a competitive basis. Shapley (1953) showed that the **Shapley Value (SV)** ψ_i^{SV} defined as follows is the only payoff method that satisfies four axioms: *efficiency*, *linearity*, *null player* and *symmetry* (see Appendix A):

$$\psi_i^{\text{SV}}(U) := \sum_{S \subseteq [n] \setminus \{i\}} \frac{|S|!(n-|S|-1)!}{n!} [U(S \cup \{i\}) - U(S)].$$

The Shapley value has a very intuitive alternative version, which this paper builds upon. Imagine that the n players join the game in some order $\pi \in \Pi$, where Π is the set of all permutations of $[n]$. Let π^i be the set of players that arrived earlier than i . Define the **random order value (ROV)** as

$$\psi_i(U) = \mathbb{E}_{\pi \sim p} [U(\pi^i \cup \{i\}) - U(\pi^i)], \quad (1)$$

where p is a distribution on Π . Going forward, we will represent each method we review or propose in terms of their p without repeating (1) (they only differ in their p ’s).

2.2. Hard Priority: Partial Order, Directed Acyclic Graph and Linear Extension

The Shapley value $\psi_i^{\text{SV}}(U)$ is the special case $p = \text{Uniform}(\Pi)$. In presence of priority, we must use a different distribution p that respects the priority relationships.

Definition 2.1 (Partial order set (poset)). A binary relation \preceq is a **partial order** if it is *reflexive* ($i \preceq i$), *antisymmetric* ($i \preceq j$ and $j \preceq i$ imply $i = j$), and *transitive* ($i \preceq j$ and $j \preceq k$ imply $i \preceq k$). The pair $([n], \preceq)$ is called a **Partially Ordered Set (poset)**. Write $i \prec j$ if $i \preceq j$ and $i \neq j$.¹

A convenient way to represent $([n], \preceq)$ is via a **Directed Acyclic Graph (DAG)**. Formally, a DAG is a graph on the node set $[n]$ with directed edges, such that for any (i, j) pair, $i \prec j$ if and only if there exists a directed path on the DAG from i to j . Throughout the paper, we use the equivalent concepts poset and DAG interchangeably for expediency.

The poset/DAG determines which permutation π ’s are valid.

Definition 2.2 (Linear extension (LE)). A permutation $\pi \in \Pi$ is a *linear extension* (LE) of the poset $([n], \preceq)$ if $i \prec j$ implies that i appears before j in π . Let Π^{\preceq} denote the set of all linear extensions on $[n]$.

Precedence Shapley Value (PSV) (Faigle & Kern, 1992). The PSV replaces the $p \sim \text{Uniform}(\Pi)$ in classical SV by $p \sim \text{Uniform}(\Pi^{\preceq})$, namely,

$$p_{\text{PSV}}(\pi) := \mathbb{1}_{[\pi \in \Pi^{\preceq}]} / |\Pi^{\preceq}|. \quad (2)$$

2.3. Soft Priority: Individual (Soft) Priority Weights

While the PSV is a very natural approach to enforce priority, it equally weights all valid linear extensions. In practice, individual players may vary in their trustworthiness, cost-convenience of data collection, potential legal risk of data use, etc. We are inclined to include trusted/low-risk data earlier in π . Notice that this consideration cannot be captured by the priority relationship (i.e., the DAG). Therefore, Kalai & Samet (1987) and Nowak & Radzik (1995) introduced individual weights $\lambda := (\lambda_1, \dots, \lambda_n)$, $\lambda_i > 0, \forall i$

¹It may be cleaner to solely define \prec . We define and base our narration on \preceq just to better connect to existing literature.

and *Weighted Shapley Value* (WSV). WSV is defined for a particular class of DAGs, called *ordered partition*.

Ordered Partition. Let (B_1, \dots, B_m) be a partition of $[n]$, i.e., $B_i \cap B_j = \emptyset, \forall 1 \leq i < j \leq m$ and $\cup_{i=1}^m B_i = [n]$. The DAG consists of edges $i \prec j$ if and only if $i \in B_r, j \in B_{r+1}$ for some $r \in [m-1]$.

In WSV, the permutation $\pi \in \Pi^{\preceq}$ is sampled in a backward fashion. To illustrate, suppose $B_1 = \{1, 2\}, B_2 = \{3, 4, 5\}$. First sample π_5 (the last element of π) from candidates 3, 4, 5 with probabilities $(\lambda_3, \lambda_4, \lambda_5) / (\lambda_3 + \lambda_4 + \lambda_5)$. Suppose 4 is selected for π_5 , then select π_4 among the remaining 3 and 5 w.p. $(\lambda_3, \lambda_5) / (\lambda_3 + \lambda_5)$, and so on. After finishing B_2 , select π_2 between 1 and 2, which also decides π_1 .

Remark 2.3. From this example, we see that λ acts as a *soft priority* parameter: a larger λ_i increases the probability that i appears later in π . This is meaningful in real applications because attribution is inherently *context dependent*: the marginal gain of adding i can be very different when the coalition already contains other (more trusted, less risky, or more “original”) contributors. Thus, increasing λ_i **does not (imprudently) directly lower i ’s payoff; instead it prefers to evaluate i under richer contexts**, which can reduce spurious early credit for noisy/duplicated/high-risk contributors while still allowing genuinely complementary contributors to remain valuable even when delayed in π .

To formalize this procedure, we define two concepts.

Definition 2.4 (Feasible set). A subset $S \subseteq [n]$ is *feasible* if $i \in S$ and $j \preceq i$ imply $j \in S$. Denote the collection of feasible sets by $\mathcal{S}^{\preceq} := \{S \subseteq [n] : S \text{ is feasible}\}$.

From Definition 2.4 onward, we slightly abuse notation: while S still denotes a subset of $[n]$, it now conforms to \preceq .

Definition 2.5 (Maximal elements). For $S \in \mathcal{S}^{\preceq}$, the set of *maximal elements*, denoted by $\max_{\preceq}(S)$, is defined as

$$\max_{\preceq}(S) := \{i \in S : \nexists j \in S \text{ s.t. } i \prec j\}.$$

Weighted Shapley Value (WSV) (Kalai & Samet, 1987; Nowak & Radzik, 1995). Write $\pi = (\pi_1, \dots, \pi_n) \in \Pi^{\preceq}$ and $S_t := \{\pi_1, \dots, \pi_t\}$, define

$$p_{\text{WSV}}(\pi) = \prod_{t=1}^n \frac{\lambda_{\pi_t}}{\sum_{j \in \max_{\preceq}(S_t)} \lambda_j}. \quad (3)$$

While WSV addresses the limitation of PSV, it only applies to special DAGs (ordered partitions), limiting its practicality.

3. Our Method

3.1. Desired Properties

Section 2 reviewed mainstream existing methods. They either (i) treat all linear extensions uniformly (PSV), capturing hard priority but no individual weighting; or (ii) incorporate weights under the strong structural assumption of ordered partitions (WSV). Our goal is to design a general approach that combines their strengths while avoiding their limitations. Specifically, we look for a $p^{(\preceq, \lambda)}$ that satisfies the following desiderata:

1. **Hard priority:** $p^{(\preceq, \lambda)}$ is supported on Π^{\preceq} .
2. **Soft priority:** when i, j are both admissible, their selection probabilities should have ratio $\lambda_i : \lambda_j$.
3. If $\lambda_i \equiv \text{constant}$, $p^{(\preceq, \lambda)}$ reduces to PSV.
4. If DAG is an ordered partition, $p^{(\preceq, \lambda)}$ reduces to WSV.
5. $p^{(\preceq, \lambda)}$ should be computationally feasible.

3.2. Priority-Aware Shapley Value (PASV)

Now we propose a $p^{(\preceq, \lambda)}$ that simultaneously captures hard precedence and player-specific weights. Our method is called **Priority-Aware Shapley Value (PASV)**.

$$p^{(\preceq, \lambda)}(\pi) \propto \prod_{t=1}^n \frac{\lambda_{\pi_t} |\max_{\preceq}(S_t)|}{\sum_{k \in \max_{\preceq}(S_t)} \lambda_k}, \quad \text{for } \pi \in \Pi^{\preceq}. \quad (4)$$

From (4), we can see how PASV combines the hard and soft priorities – while restricting π to Π^{\preceq} enforces the hard priority, the soft priorities of admissible candidates for each π_t is adjusted by λ_i ’s, thus reflecting the soft priority. When λ_i ’s are all equal, (4) becomes $p^{(\preceq, \lambda)}(\pi) \propto 1$, and PASV recovers PSV. When the DAG is an ordered partition, it can be shown that $p^{(\preceq, \lambda)}(\pi) = \prod_{t=1}^n \frac{\lambda_{\pi_t}}{\sum_{k \in \max_{\preceq}(S_t)} \lambda_k}$, thus recovering WSV. Formally, we have the following results.

Proposition 3.1 (Reduction to PSV). *If $\lambda_1 = \dots = \lambda_n$, then $p^{(\preceq, \lambda)}(\pi) = p_{\text{PSV}}(\pi), \forall \pi \in \Pi^{\preceq}$.*

Proposition 3.2 (Reduction to WSV). *If the DAG is an ordered partition, then $p^{(\preceq, \lambda)}(\pi) = p_{\text{WSV}}(\pi), \forall \pi \in \Pi^{\preceq}$.*

Remark 3.3. When developing a general $p^{(\preceq, \lambda)}$, one may be tempted to directly apply the formulation of WSV (3) to general DAGs, but the resulting distribution does not reduce to PSV for equal weights. The $|\max_{\preceq}(S_t)|$ factor on the numerator of (4) is crucial for ensuring Proposition 3.1.

PASV can also be efficiently computed. We relegate the algorithm details to the dedicated Section 4.

3.3. Axiomatization of PASV

Like SV, PSV and WSV, our PASV can also be naturally derived from a set of axioms. Here, we provide readers an outline as a preview of this axiomatization. Notice that it contains acronyms and jargon that will be defined later.

- Axioms $E + L + NP + M + MS \Rightarrow PROV$ (a big family)
- Focus on “**SCF form**” to narrow down PROV
- Add axioms **WP + EWU** to align with boundary cases

Finally, $PROV + SCF + WP + EWU \Rightarrow PASV$. Next, we carry out and elaborate this outline.

3.3.1. PRECEDENCE RANDOM ORDER VALUE (PROV)

Recall that the classical Shapley value can be rewritten as a random order value (ROV). In presence of priority, we should of course constrain our consideration to p distributions supported not on all of Π , but on the subset $\Pi^{\preceq} \subseteq \Pi$ that respects priority.

Definition 3.4 (Precedence random order value (PROV)). A value ψ is called a **precedence random order value (PROV)** if there exists some p supported on Π^{\preceq} , s.t. $\psi_i(U) = \mathbb{E}_{\pi \sim p} [U(\pi^i \cup \{i\}) - U(\pi^i)]$ for all U and i .

While it may be natural to treat PROV as a basic assumption or an axiom, we will show that in fact PROV can be derived from five more basic axioms. These axioms include three Shapley axioms: Efficiency (E), Linearity (L) and Null player (NP) (see Appendix A); plus two more axioms: Monotonicity (M) and Maximal support (MS).

Axiom 3.5 (Monotonicity). If U is *monotone*, i.e., $S \subseteq T \Rightarrow U(S) \leq U(T)$ for all $S, T \subseteq [n]$, then every player receives a nonnegative payoff: $\psi_i(U) \geq 0$ for all $i \in [n]$.

Weber (1988) showed that axioms $E + L + NP + M \Rightarrow ROV$. Since PROV is a special ROV, it naturally inherits these axioms. To present axiom MS, we first define *elementary game* – it has long been used for analyzing Shapley’s values.

Definition 3.6 (Elementary game). For a given subset $T \subseteq [n]$, the *elementary game* $u_T \in \Gamma$ on T is defined by $u_T(S) := \mathbb{1}\{T \subseteq S\}$ for $S \subseteq [n]$.

We focus on elementary games for feasible T , i.e., $T \in \mathcal{S}^{\preceq}$ (recall Definition 2.4). The precedence relation singles out the *maximal* elements of T as sole the recipients of credit. This motivates the following axiom.

Axiom 3.7 (Maximal support). For any elementary game u_T with $T \in \mathcal{S}^{\preceq}$, if player i is not maximal in T , i.e., $i \notin \max_{\preceq}(T)$, then $\psi_i(u_T) = 0$.

Theorem 3.8 (Axiomatization of PROV). A value ψ is **PROV** \Leftrightarrow it satisfies axioms $E + L + NP + M + MS$.

3.3.2. STATE-CHOICE FACTORIZATION (SCF)

The PROV as defined in Definition 3.4 is a huge family, and using the most general PROV directly is computationally challenging. We therefore restrict attention to a broad and structured family of precedence-respecting order distributions that factorize along the chain of feasible sets induced by a linear extension. Conceptually, this is the precedence-constrained analogue of stage-wise models for rankings and permutations, such as the Plackett–Luce (Luce et al., 1959; Plackett, 1975) and multistage ranking families (Fligner & Verducci, 1988). To this end, we consider the family of distributions on Π^{\preceq} of the form

$$p(\pi) \propto \prod_{t=1}^n w_{\preceq, \lambda}(\pi_t; S_t), \quad \text{for } \pi \in \Pi^{\preceq} \quad (5)$$

for some $w_{\preceq, \lambda}$. This form (5) is the precedence-constrained analogue of Plackett-Luce: the likelihood of some π depends on π only through the sequence of feasible candidates $\{S_t\}_{t=1}^n$, and the chosen candidate at this time. It is often convenient to decompose w as a *scale* (“state”): $s_{\preceq}(S_t) := \sum_{k \in \max_{\preceq}(S_t)} w_{\preceq, \lambda}(k; S_t)$, where we shall further assume that $s_{\preceq}(S_t)$ does not depend on λ , which is true for WSV; and a *normalized priority weighting* (“choice”): $c_{\preceq, \lambda}(i; S_t) := w_{\preceq, \lambda}(i; S_t) / s_{\preceq}(S_t)$.

Definition 3.9 (State–Choice Factorization (SCF)). For a poset $([n], \preceq)$, define the prefix (remaining) set $S_t = \{\pi_1, \dots, \pi_t\}$ as a chain of feasible sets ($t = n, n-1, \dots, 1$). A **state–choice factorization (SCF)** assigns an unnormalized weight to π by multiplying:

- i) a **state factor** $s_{\preceq}(S_t)$ that captures global bias induced by the precedence structure;
- ii) a **choice factor** $c_{\preceq, \lambda}(\cdot; S)$ that encodes soft priority weighting of admissible candidates $\max_{\preceq}(S)$; it is the entry point for the individual weights λ .

Formally, an SCF p has the following form

$$p(\pi) \propto \prod_{t=1}^n s_{\preceq}(S_t) c_{\preceq, \lambda}(\pi_t; S_t), \quad \text{for } \pi \in \Pi^{\preceq}, \quad (6)$$

where $\sum_{i \in \max_{\preceq}(S_t)} c_{\preceq, \lambda}(i; S_t) = 1$.

The merits of SCF are three-fold:

- It remains flexible enough to capture a broad range of precedence-respecting random-order models, containing PSV and WSV as special cases.
- It preserves a clear interpretation of λ weights as a soft priority parameter;
- Its factorization form enables efficient MCMC sampling procedures for generating π .

3.3.3. BOUNDARY CASE AXIOMS

We desire our method to contain PSV and WSV as special cases. This is characterized by the following two axioms.

Axiom 3.10 (Weight Proportionality). For every feasible set $S \in \mathcal{S}^{\preceq}$ and every $i, j \in \max_{\preceq}(S)$, $\frac{c_{\preceq, \lambda}(i; S)}{c_{\preceq, \lambda}(j; S)} = \frac{\lambda_i}{\lambda_j}$.

Axiom WP requires that at each step the probability of choosing each admissible candidate i is proportional to λ_i .

Axiom 3.11 (Equal-Weight Uniformity). If $\lambda_i \equiv c$ for all $i \in [n]$, then the induced distribution is uniform on Π^{\preceq} .

Axiom 3.10 recovers WSV and Axiom 3.11 recovers PSV.

3.3.4. AXIOMATIZATION OF PASV

Theorem 3.12. Suppose p is a PROV as in Definition 3.4 satisfying the SCF form as in (6). Then the only p that also satisfies Axioms 3.10 and 3.11 is PASV as defined in (4).

3.4. Limiting Cases of the Priority-Aware Distribution

This section studies what happens to the PASV order distribution when a player weight becomes extreme. The goal is to clarify how the *soft* priorities encoded by λ interact with the *hard* precedence constraints \preceq (equivalently, the DAG). In PASV (4), λ affects the distribution only through the choice factor $c_{\preceq, \lambda}(i; S)$ over the currently admissible (maximal) set $\max_{\preceq}(S)$. For $i \in \max_{\preceq}(S)$, we have

$$c_{\preceq, \lambda}(i; S) = \frac{\lambda_i}{\lambda_i + \sum_{k \in \max_{\preceq}(S) \setminus \{i\}} \lambda_k}. \quad (7)$$

If $\max_{\preceq}(S) = \{i\}$, changing λ_i has no effect. When $|\max_{\preceq}(S)| \geq 2$ all other weights are held fixed, (7) implies $c_{\preceq, \lambda}(i; S) \rightarrow 1$ as $\lambda_i \rightarrow \infty$ and $c_{\preceq, \lambda}(i; S) \rightarrow 0$ as $\lambda_i \rightarrow 0^+$. In other words, **extreme weights induce an (almost) deterministic tie-break among simultaneously admissible players**: $\lambda_i \rightarrow \infty$ selects i whenever it is maximal, i.e., pushing i as *late* as allowed in π (in the forward order), while $\lambda_i \rightarrow 0^+$ pulls i as *early* as possible in π .

Interestingly, in some cases, extreme weights can simply translate into new DAG edges. We showcase two scenarios: (i) the extreme-weight player is globally maximal, and (ii) DAG is an ordered partition. Figure 2 illustrates two examples. Importantly, we emphasize the following takeaways.

- These new edges will **not** create cycles; and
- Setting weights in whatever way will **not** delete, rewire or reverse existing edges in the original DAG.

Formally, we have the following theoretical results.

Proposition 3.13. Fix a poset $([n], \preceq)$ and $i \in \max_{\preceq}([n])$, let \preceq' be the partial order obtained by adding $j \prec i$ for all

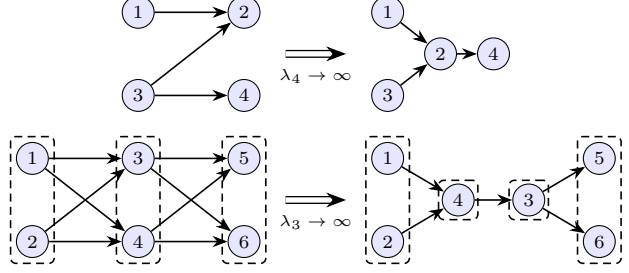


Figure 2. Extreme λ may translate into DAG edges: Top: sending $\lambda_4 \rightarrow \infty$ adds an edge $2 \rightarrow 4$ (on the right we omitted the edge $3 \rightarrow 4$ as it is implied by the path $3 \rightarrow 2 \rightarrow 4$). Bottom: sending $\lambda_3 \rightarrow \infty$ adds an edge $4 \rightarrow 3$, forming a refined layer structure.

$j \in \max_{\preceq}([n]) \setminus \{i\}$. Then for any λ' satisfying $\lambda'_j = \lambda_j$ for all $j \neq i$ (with arbitrary $\lambda'_i > 0$), and for every $\pi \in \Pi$,

$$\lim_{\lambda_i \rightarrow \infty} p^{(\preceq, \lambda)}(\pi) = p^{(\preceq', \lambda')}(\pi) \cdot \mathbb{1}_{[\pi \in \Pi^{\preceq'}]}.$$

Proposition 3.14. Assume \preceq is an ordered partition (B_1, \dots, B_m) . Fix a layer $B \in \{B_1, \dots, B_m\}$ and a nonempty subset $G \subseteq B$. Fix weights $(\lambda_j)_{j \notin G}$ and consider the regime in which $\lambda_i = \bar{\lambda}$ for all $i \in G$ while $\bar{\lambda} \rightarrow \infty$. Let \preceq' represent the refined ordered partition obtained by splitting B into two ordered, consecutive layers $(B \setminus G, G)$. Then for any λ' satisfying $\lambda'_j = \lambda_j$ for all $j \notin G$ and $\lambda_i = \tilde{\lambda}$ for $i \in G$ with arbitrary $\tilde{\lambda} > 0$, and for every $\pi \in \Pi$,

$$\lim_{\bar{\lambda} \rightarrow \infty} p^{(\preceq, \lambda)}(\pi) = p^{(\preceq', \lambda')}(\pi) \mathbb{1}_{[\pi \in \Pi^{\preceq'}]}.$$

More broadly, however, extreme weights are *not* equivalent to adding a fixed set of edges in general. The key reason is that the tie-break is triggered only when the extreme-weight player becomes maximal, and *whether/when* this happens depends on the realized history of the (backward) construction of π . Figure 3 gives a counterexample.

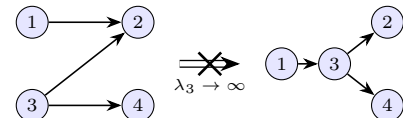


Figure 3. Extreme λ may not always translate into a new DAG edge: if $\pi_4 = 2$, then 1 and 4 are both eligible for π_3 ; the (only possible) edge to add 1 \rightarrow 3 would incorrectly deny 1's candidacy.

Priority sweeping. Beyond producing a single valuation, PASV enables a handy sensitivity/robustness test w.r.t. λ . Fixing the DAG and a baseline λ , for each player i , our **priority sweeping** tracks how the valuation of i changes as λ_i varies in $(0, \infty)$. This would tell us which players' values are stable versus sensitive to its weight.

4. Computation Algorithm for PASV

Recall that PASV is defined in an ROV form as in (1), where $p = p_{\text{PASV}}$ as in (4). While the expectation in (1) can be

easily approximated by a Monte Carlo sampling with i.i.d. $\pi \sim p_{\text{PASV}}$, the main computational challenge lies exactly in how to sample π from the distribution p_{PASV} , because the number of valid π 's grows exponentially with n . Practical computation therefore typically relies on Markov Chain Monte Carlo (MCMC) strategies.

Adjacent-swap M-H on Π^{\preceq} . The common approach to MCMC on Π^{\preceq} is via *adjacent swaps* of incomparable neighbors (Karzanov & Khachiyan, 1991; Bubley & Dyer, 1999). We adopt this method but generalize the uniform distribution to $p^{(\preceq, \lambda)}(\cdot)$. To start, it is not difficult to find one valid $\pi \in \Pi^{\preceq}$ as the initialization (Kahn, 1962). Then in each iteration, sample $k \in [n-1]$ at random. If (π_k, π_{k+1}) are *incomparable*, i.e., neither of π_k, π_{k+1} precedes the other, propose π' by swapping them; otherwise, stay at π . The Metropolis–Hastings (M-H) acceptance probability is

$$\alpha := \mathbb{P}(\pi \rightarrow \pi') = \min \left\{ 1, p^{(\preceq, \lambda)}(\pi') / p^{(\preceq, \lambda)}(\pi) \right\}. \quad (8)$$

Although $p^{(\preceq, \lambda)}(\cdot)$ is defined as a product over n steps, the acceptance ratio in (8) can be evaluated using only local information around chosen position k .

Lemma 4.1. Fix a poset $([n], \preceq)$ and weights λ . Let $\pi \in \Pi^{\preceq}$ and fix $k \in [n-1]$ such that π_k and π_{k+1} are incomparable. Let π' be the permutation obtained by swapping (π_k, π_{k+1}) in π . Then we have

$$\frac{p^{(\preceq, \lambda)}(\pi')}{p^{(\preceq, \lambda)}(\pi)} = \frac{(\sum_{i \in M_k} \lambda_i) / |M_k|}{(\sum_{j \in M'_k} \lambda_j) / |M'_k|}, \quad (9)$$

where $M_k = \max_{\preceq}(S_k)$, $M'_k = \max_{\preceq}(S'_k)$, $S_k = \{\pi_t\}_{t \in [k]}$, and $S'_k = \{\pi_t\}_{t \in [k-1] \cup \{k+1\}}$.

Algorithm 1 describes our algorithm for sampling $\pi \sim p_{\text{PASV}}$. Based on Algorithm 1, PASV can be efficiently approximated by a Monte Carlo on (1) without difficulty.

5. Experiments

5.1. PASV for Data Valuation

We evaluate PASV in a data market setting with explicit *data lineage* (some providers' training examples are derived or copied from others), comparing it against existing methods.

Setup: data and utility. We use MNIST (LeCun et al., 2002) and CIFAR10 (Krizhevsky et al., 2009), both containing 10 classes, with a k -NN classifier (MNIST: pixel features; CIFAR10: pretrained ResNet-18 embeddings (He et al., 2016)). We fix a balanced test set of size 1000 (100 per class) and define the utility of a training subset S as test accuracy, $U(S)$. We consider eight data providers, each contributing 100 training data points ($n = 800$ players (data points) in total):

Algorithm 1 M-H algorithm for sampling $\pi \sim p^{(\preceq, \lambda)}(\cdot)$.

```

Input: poset  $([n], \preceq)$ ; weights  $\lambda$ ; number of samples  $N_{\text{MC}}$ ; burn-in  $B$ ; thinning  $\tau$ ; index sampler  $f$  on  $[n-1]$ .
Initialize  $\pi^{(0)} \in \Pi^{\preceq}$ ; Set of sampled  $\pi$ 's:  $\mathcal{T} \leftarrow \emptyset$ 
for  $t = 1$  to  $B + \tau(N_{\text{MC}} - 1) + 1$  do
    Draw  $k \sim f$ ; set  $\pi \leftarrow \pi^{(t-1)}$ 
    if  $\pi_k$  and  $\pi_{k+1}$  are incomparable then
         $\pi' \leftarrow (\pi \text{ with } (\pi_k, \pi_{k+1}) \text{ swapped})$ 
        Compute  $(S_k, S'_k, M_k, M'_k)$  and  $\alpha$ , c.f. (8), (9)
        With prob.  $\alpha$ , set  $\pi^{(t)} \leftarrow \pi'$ ; otherwise set  $\pi^{(t)} \leftarrow \pi$ 
    else
         $\pi^{(t)} \leftarrow \pi$ 
    end if
    if  $t > B$  and  $(t - B - 1) \bmod \tau = 0$  then
        Append  $\pi^{(t)}$  to  $\mathcal{T}$ 
    end if
end for
return  $\mathcal{T}$ 

```

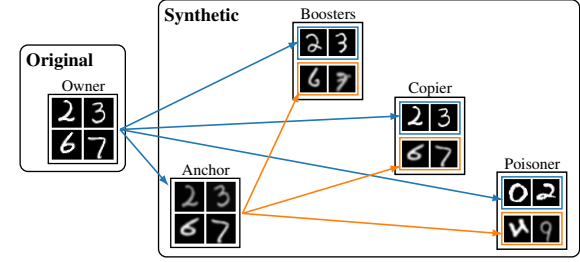


Figure 4. The DAG used for MNIST/CIFAR10. Only one Booster is shown. Here, (for example) a blue edge from Owner to half of Copier represents 100×50 edges between their members.

- **Owner:** original labeled data points.
- **Anchor:** classical augmentation applied to Owner (e.g., rotation/blur); producing synthetic data points that downstream providers may reuse.
- **Four Boosters:** four generative model families, GAN (Goodfellow et al., 2020), DDPM (Ho et al., 2020), DDIM (Song et al., 2020), and FM (Lipman et al., 2022) that produce synthetic data points. Each Booster contributes 50 samples from a genAI model trained on Owner and another 50 samples trained on Anchor.
- **Copier:** copies half from Owner and half from Anchor.
- **Poisoner:** copies the same way as Copier but randomly flips labels (harmful reuse).

Data lineage and DAG. We encode data lineage as a precedence DAG over *blocks*. Owner and Anchor each form a block. For every reuse-based provider (4 Boosters, Copier, Poisoner), we split its data into two blocks: Owner-derived vs. Anchor-derived. This yields a 14 block-DAG (which is not an ordered partition), illustrated in Figure 4.

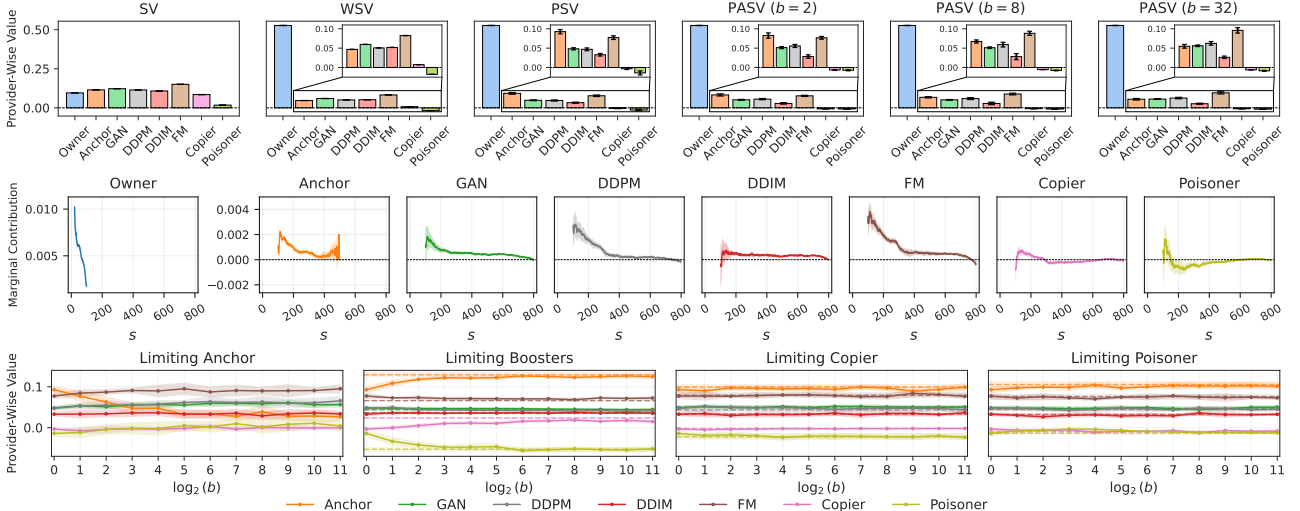


Figure 5. MNIST results. **Top:** Provider-level values (summed value for each provider (Lee et al., 2025); 10 repetitions, report mean & ± 1 std. bars; **Middle:** Marginal contributions: $\mathbb{E}[U(\pi^i \cup \{i\}) - U(\pi^i) | |\pi^i| = s]$ vs s , c.f. (1), $p := \text{Uniform}(\Pi^{\preceq})$; **Bottom:** Priority sweeping: $c \in \{(0, 1, 0, 0, 0), \dots, (0, 0, 0, 0, 1)\}$, $b \in \{2^k : k \in [11]\}$, Owner not swept (alone in maximal set, weight has no effect).

Benchmarks. (i) **classical SV** (Ghorbani & Zou, 2019); (ii) **WSV**: approximate the DAG by a two-layer ordered-partition: Original (Owner) \prec Synthetic (Anchor, Boosters, etc) (Zheng et al., 2025); (iii) **PSV** (Faigle & Kern, 1992).

Soft priority weights. We set individual weights according to their provider type as $\lambda = b^c$, with a shared base $b > 1$ and exponents $c = (c_{\text{Owner}}, c_{\text{Anchor}}, c_{\text{Booster}}, c_{\text{Copier}}, c_{\text{Poisoner}})$.

Main comparison. We first conduct a *main comparison*, in which $c = (0, 1, 0, 2, 2)$ and $b \in \{2, 8, 32\}$, mildly penalizing Anchor and more strongly penalizing Copier/Poisoner. Here, we use weights to softly incorporate our prior knowledge of *usefulness*, e.g., anticipating that the test set might not necessarily feature rotated images as seen in Anchor, our λ favored Boosters over Anchor, since Boosters contain data generated directly based on Owner without excess rotation.

Row 1 of Figure 5 reports *provider-level* results for MNIST (CIFAR10 in Appendix B.1.3). SV over-credits data reuse (e.g., Copier), as it ignores precedence. WSV favors Owner by forcing “Original \prec Synthetic” but still mixes up among synthetic providers due to its structural limitation (Anchor is less credited, positive values for Copier). PSV better preserves credit for upstream sources and can reveal negative value for Copier. PASV then provides a more flexible controlled adjustment: increasing b progressively suppresses the penalized types (Anchor/Copier/Poisoner) while respecting the same reuse constraints as PSV.

To better understand the effect of priority sweeping in PASV relative to PSV, we examine how a data point’s marginal gain depends on its entry position in π . In PASV, data points with larger λ_j are more likely to be evaluated at later posi-

tions, when permitted by the DAG (see Remark 2.3). We therefore plot the average marginal gain conditional on entering at each position s for each data provider. Row 2 of Figure 5 shows the marginal-gain curves and offers insights (c.f. caption of Figure 5). Anchor and 4 Boosters show similar trends: the earlier in π the more significant the recognition of their positive contributions, and FM showed the most prominent trend. These position-dependent patterns explain the difference between PSV and PASV observed in Row 1. PASV tends to evaluate data from Anchor, Copier, and Poisoner in richer coalition contexts and thus places more weight on their tail-regime marginal gains, leading to more diminished final valuations.

Interestingly, Copier/Poisoner both show a “positive spike” for small $|\pi^i|$; this is because when $|\pi^i| \approx 100$, the sampled size from each class (on average just 10) may be unstable; in this situation, adding copied or even noisy data may still benefit the numerical stability of the classifier: when a class has few members present in a small π^i , adding Copier data can help k -NN avoid drawing neighbors from other classes.

Sensitivity analysis. Row 3 of Figure 5 shows how provider-level valuations vary as b grows for each of Anchor/Booster/Copier/Poisoner with their own indicator c , c.f. caption of Figure 5. Applying our theoretical result in Section 3.4, we predict that as $b \rightarrow \infty$, for each of Boosters/Copier/Poisoner, we can compute a PSV with the DAG with added edges incoming from other providers (e.g., the analysis for Boosters sets $c = (0, 0, 1, 0, 0)$, then $b \rightarrow \infty$ is equivalent to adding edges $\{\text{Copier}, \text{Poisoner}\} \rightarrow \text{Boosters}$). In Row 3 plots, we used dashed lines to mark the PASV computed under the new DAG with added edges, and they well-corroborate observed PASV values for large b , vali-

dating our theory’s prediction. However, this simplified translation does not apply to Anchor for the same reason as the example in Figure 3.

5.2. Application to Feature Attribution

While priority relations are usually considered for data Shapley, in feature Shapley, domain knowledge may require certain variables to be considered before others (e.g., causal ancestors before descendants) (Frye et al., 2020). Here we test PASV in an attribution setting with precedence constraints encoded by a general DAG and focus on the attribution sensitivity to: (i) DAG; and (ii) priority weights.

Setup. We follow Frye et al. (2020) on the UCI Census Income (Adult) dataset (Asuncion et al., 2007), predicting whether annual income exceeds \$50K. We remove `fnlwgt` and `education-num` to avoid redundancy, leaving $n = 12$ features as players. We train a two-hidden-layer MLP with 100 units per layer.

Utility function. For a predictor f , let $f_y(x)$ denote the predicted probability of assigning an input x to the (true) class y . For any subset of features $S \subseteq [n]$, we first use a k -NN imputation procedure (detailed steps in Appendix B.2.1) to estimate $u_S(x, y) = \mathbb{E}_{x' \sim p(x'|x_S)} [f_y(x_S \oplus x'_{S^c})]$ (Janzing et al., 2020; Sundararajan & Najmi, 2020; Frye et al., 2021). Then we can define the utility function as $U(S) = \mathbb{E}_{(x, y) \sim p(x, y)} [u_S(x, y)]$ and approximate it by empirically sampling (x, y) from the original data.

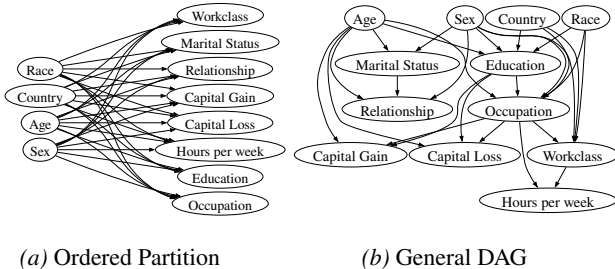


Figure 6. Two DAG specifications over the 12 income features.

DAG specification. Figure 6 compares two DAGs encoding which feature orders are admissible. The first is a coarse ordered partition used by Frye et al. (2020), where four demographic variables precede the rest (Figure 6a). The second is a more detailed precedence DAG over the same 12 features (Figure 6b) that adds AI-suggested additional relations based on common sense and domain knowledge (e.g., education \prec occupation); details in Appendix B.2.3.

Experimental procedure. For each DAG, we first compute PASV with uniform weights $\lambda_i \equiv 1$, which reduces to PSV. For the ordered-partition DAG, this also coincides with

the uniform-weight WSV; for the general DAG, computing PSV/PASV requires the MCMC sampler in Section 4. Next, we perform a *priority sweeping*: for each feature i , vary $\lambda_i \in \{2^k : k \in [-8 : 8]\}$ while holding $\lambda_j \equiv 1, \forall j : j \neq i$.

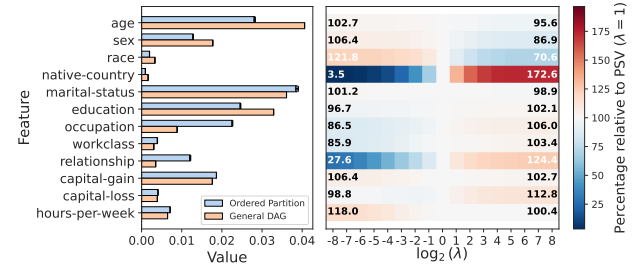


Figure 7. Results of feature attribution for Census Income dataset. (Left) PSV (=PASV) under the two DAGs with uniform weights. (Right) Sensitivity analysis using priority sweeping.

Results. Figure 7 highlights two takeaways. First, the left panel shows that **DAG matters a lot**: with the same utility function, the PSV valuation changes noticeably between ordered partition and the richer DAG, indicating that using a coarse DAG (e.g., ordered partition) may significantly alter results. Second, the priority sweeping with our PASV in the right panel **provides a crucial sensitivity diagnosis**. For example, several demographic variables (age, sex, race) decrease when delayed (large λ), whereas others (e.g., native-country, relationship, occupation) increase, and some features exhibit non-monotone responses. This is consistent with the intuitive understanding in Section 5.1: moving a feature later changes the set of variables already present when its marginal contribution is evaluated, so the effect depends on whether the feature is redundant with, or complementary to, its typical competitors under the assumed DAG. Overall, PASV’s priority sweeping provides a practical diagnostic tool for identifying which attributions are robust to priority weighting (e.g., marital-status, capital-loss, etc) and which are unstable (most noticeably native-country and relationship).

6. Conclusion

We introduce Priority-Aware Shapley Value (PASV), a unified Shapley-based attribution method that simultaneously enforces hard precedence constraints and incorporates soft priority weights. PASV recovers precedence-only and weight-only Shapley variants as special cases, admits scalable MCMC estimation for general DAGs, and has a solid axiomatization basis. An important tool that PASV provides practitioners is a sensitivity/robustness diagnostic procedure via *priority sweeping*.

Impact Statement

This paper presents work whose goal is to advance the field of Machine Learning. There are many potential societal consequences of our work, none of which we feel must be specifically highlighted here.

Acknowledgements

Lee and Zhang were supported by NSF DMS-2311109. Liu and Tang were supported by NSF DMS-2412853 and Jane Street Group, LLC.

References

Aas, K., Jullum, M., and Løland, A. Explaining individual predictions when features are dependent: More accurate approximations to Shapley values. *Artificial Intelligence*, 298:103502, 2021.

Asuncion, A., Newman, D., et al. UCI machine learning repository, 2007.

Bubley, R. and Dyer, M. Faster random generation of linear extensions. *Discrete mathematics*, 201(1-3):81–88, 1999.

Faigle, U. and Kern, W. The Shapley value for cooperative games under precedence constraints. *International Journal of Game Theory*, 21(3):249–266, 1992.

Falconer, T., Kazempour, J., and Pinson, P. Toward replication-robust analytics markets. *INFORMS Journal on Data Science*, 2025.

Fligner, M. A. and Verducci, J. S. Multistage ranking models. *Journal of the American Statistical association*, 83 (403):892–901, 1988.

Frye, C., Rowat, C., and Feige, I. Asymmetric Shapley values: incorporating causal knowledge into model-agnostic explainability. *Advances in neural information processing systems*, 33:1229–1239, 2020.

Frye, C., de Mijolla, D., Begley, T., Cowton, L., Stanley, M., and Feige, I. Shapley explainability on the data manifold. In *International Conference on Learning Representations*, 2021.

Ghorbani, A. and Zou, J. Data shapley: Equitable valuation of data for machine learning. In *International conference on machine learning*, pp. 2242–2251. PMLR, 2019.

Goodfellow, I., Pouget-Abadie, J., Mirza, M., Xu, B., Warde-Farley, D., Ozair, S., Courville, A., and Bengio, Y. Generative adversarial networks. *Communications of the ACM*, 63(11):139–144, 2020.

Han, D., Wooldridge, M., Rogers, A., Ohrimenko, O., and Tschiatschek, S. Replication robust payoff allocation in submodular cooperative games. *IEEE Transactions on Artificial Intelligence*, 4(5):1114–1128, 2022.

He, K., Zhang, X., Ren, S., and Sun, J. Deep residual learning for image recognition. In *Proceedings of the IEEE conference on computer vision and pattern recognition*, pp. 770–778, 2016.

Ho, J., Jain, A., and Abbeel, P. Denoising diffusion probabilistic models. *Advances in neural information processing systems*, 33:6840–6851, 2020.

Janzing, D., Minorics, L., and Blöbaum, P. Feature relevance quantification in explainable ai: A causal problem. In *International Conference on artificial intelligence and statistics*, pp. 2907–2916. PMLR, 2020.

Kahn, A. B. Topological sorting of large networks. *Communications of the ACM*, 5(11):558–562, 1962.

Kalai, E. and Samet, D. On weighted Shapley values. *International journal of game theory*, 16(3):205–222, 1987.

Karzanov, A. and Khachiyan, L. On the conductance of order Markov chains. *Order*, 8(1):7–15, 1991.

Krizhevsky, A., Hinton, G., et al. Learning multiple layers of features from tiny images. 2009.

Kwon, Y. and Zou, J. Beta shapley: a unified and noise-reduced data valuation framework for machine learning. *arXiv preprint arXiv:2110.14049*, 2021.

LeCun, Y., Bottou, L., Bengio, Y., and Haffner, P. Gradient-based learning applied to document recognition. *Proceedings of the IEEE*, 86(11):2278–2324, 2002.

Lee, K., Liu, Z., Tang, W., and Zhang, Y. Faithful group Shapley value. In *The Thirty-ninth Annual Conference on Neural Information Processing Systems*, 2025.

Lipman, Y., Chen, R. T., Ben-Hamu, H., Nickel, M., and Le, M. Flow matching for generative modeling. *arXiv preprint arXiv:2210.02747*, 2022.

Luce, R. D. et al. *Individual choice behavior*, volume 4. Wiley New York, 1959.

Lundberg, S. M. and Lee, S.-I. A unified approach to interpreting model predictions. *Advances in neural information processing systems*, 30, 2017.

Mersha, M., Lam, K., Wood, J., Alshami, A. K., and Kalita, J. Explainable artificial intelligence: A survey of needs, techniques, applications, and future direction. *Neurocomputing*, 599:128111, 2024.

Nowak, A. S. and Radzik, T. On axiomatizations of the weighted Shapley values. *Games and Economic Behavior*, 8(2):389–405, 1995.

Plackett, R. L. The analysis of permutations. *Journal of the Royal Statistical Society Series C: Applied Statistics*, 24(2):193–202, 1975.

Shapley, L. S. A value for n -person games. *Contributions to the Theory of Games*, 2, 1953.

Song, J., Meng, C., and Ermon, S. Denoising diffusion implicit models. *arXiv preprint arXiv:2010.02502*, 2020.

Sundararajan, M. and Najmi, A. The many Shapley values for model explanation. In *International conference on machine learning*, pp. 9269–9278. PMLR, 2020.

Wang, J. T. and Jia, R. Data Banzhaf: A robust data valuation framework for machine learning. In *International Conference on Artificial Intelligence and Statistics*, pp. 6388–6421. PMLR, 2023.

Weber, R. J. *Probabilistic values for games*, pp. 101–120. Cambridge University Press, 1988.

Wu, M., Jia, R., Lin, C., Huang, W., and Chang, X. Variance reduced Shapley value estimation for trustworthy data valuation. *Computers & Operations Research*, 159:106305, 2023.

Zha, D., Bhat, Z. P., Lai, K.-H., Yang, F., Jiang, Z., Zhong, S., and Hu, X. Data-centric artificial intelligence: A survey. *ACM Computing Surveys*, 57(5):1–42, 2025.

Zheng, X., Huang, Y., Chang, X., Jia, R., and Tan, Y. Rethinking data value: Asymmetric data Shapley for structure-aware valuation in data markets and machine learning pipelines. *arXiv preprint arXiv:2511.12863*, 2025.

A. Standard Axioms of the Shapley Value

We briefly review the standard axiomatic framework leading to the Shapley value. Throughout this appendix we fix the player set $[n] = \{1, \dots, n\}$ and assume $U(\emptyset) = 0$ without loss of generality, since replacing U by $U'(S) := U(S) - U(\emptyset)$ leaves every marginal contribution $U(S \cup \{i\}) - U(S)$ unchanged. A *value* is a mapping ψ that assigns to each utility function U a payoff vector $\psi(U) = (\psi_i(U))_{i \in [n]}$. The Shapley value ψ^{SV} is characterized as the unique value satisfying the following four standard axioms (Shapley, 1953).

Axiom A.1 (Efficiency; E). For a given utility function U ,

$$\sum_{i \in [n]} \psi_i(U) = U([n]).$$

Axiom A.2 (Linearity; L). For given two utility functions U, V and all $\alpha, \beta \in \mathbb{R}$,

$$\psi(\alpha U + \beta V) = \alpha\psi(U) + \beta\psi(V).$$

Axiom A.3 (Null Player; NP). If player i satisfies $U(S \cup \{i\}) = U(S)$ for all $S \subseteq [n] \setminus \{i\}$, then

$$\psi_i(U) = 0.$$

Axiom A.4 (Symmetry; S). If two players i and j satisfy $U(S \cup \{i\}) = U(S \cup \{j\})$ for all $S \subseteq [n] \setminus \{i, j\}$, then

$$\psi_i(U) = \psi_j(U).$$

Efficiency requires that the entire value $U([n])$ be fully allocated among players. Linearity ensures that payoffs respect additive changes in utility. That is, if a game is formed by combining (possibly with weights) two utilities, then the assigned payoffs combine in the same way. Null player formalizes a fairness requirement in the sense of that a player who never changes the utility receives zero payoff. Symmetry reflects anonymity by requiring identical treatment of players who are interchangeable in terms of their marginal contributions.

B. Additional Experimental Details

This appendix provides additional experimental details and results for the main paper. We present two experimental settings in which we apply PASV for data valuation and feature attribution. The data valuation experiments study provider-level values under the priority structure described in Section 5.1. The feature attribution experiments examine how precedence constraints shape feature attributions in Section 5.2.

All experiments were run on a shared computing cluster, provided by the College of Arts and Sciences at The Ohio State University. Generative AI training and sampling in Section 5.1 used one NVIDIA V100 GPU with 32 GB VRAM per run. All other experiments were performed on CPU nodes with allocated resources fixed at 16 CPU cores and 32 GB RAM per run, using various Intel Xeon processors.²

B.1. Experiment in Section 5.1

B.1.1. DETAILED SETUP

We provide additional implementation details for the data valuation experiments in Section 5.1. The random seed was fixed for dataset construction, and value estimation was replicated across 10 independent random seeds. We report the mean and one standard deviation across these runs.

Utility was defined as the test accuracy of a k -NN classifier with Euclidean distance using $k = 20$. For CIFAR10, we used ImageNet-pretrained ResNet-18 features, extracting the 512-dimensional representation from the global average pooling output immediately before the final fully connected layer. Each CIFAR10 image was normalized using ImageNet statistics prior to feature extraction, and the resulting embeddings were ℓ_2 -normalized.

Provider datasets were constructed as follows. The **Owner** dataset was sampled from the original dataset with balanced class proportions. The **Anchor** dataset was obtained by applying geometric and optical augmentations to the Owner samples. Each augmentation parameter was sampled independently from a uniform distribution over the stated range.

²Jobs could be placed on different nodes depending on cluster availability, so the specific CPU model varied across runs.

- Scaling in $[0.95, 1.05]$
- Brightness in $[0.7, 1.3]$ for MNIST, and in $[0.8, 1.2]$ for CIFAR10
- Contrast in $[0.7, 1.3]$ for MNIST, and in $[0.8, 1.2]$ for CIFAR10
- Translation sampled independently in the horizontal and vertical directions, each by up to $1/32$ of the image size.
- Rotation in $[-15^\circ, 15^\circ]$ for MNIST
- For MNIST, Gaussian blur with kernel size 3 and $\sigma \in [0.5, 1.5]$.
- For CIFAR10, horizontal flip with probability 0.5.

For each **Booster**, we trained a class-conditional generative model on the Owner dataset, and also trained a second model on the Anchor-augmented version of the Owner dataset. We then sampled a class-balanced set of size $n/2$ from each model via label conditioning. Full generative model specifications are provided in Appendix B.1.2. The **Copier** dataset was formed by copying half of the Owner samples while preserving class balance, and likewise half of the Anchor samples. The **Poisoner** dataset was formed by taking half of the Owner samples with balanced class proportions and replacing each label with a uniformly sampled incorrect class label, and likewise for half of the Anchor samples.

All values were estimated via Monte Carlo using $N_{MC} = 10,000$ samples. For PASV, we sampled linear extensions using Algorithm 1 with burn-in $B = 100,000$ and thinning $\tau = 10,000$. The index proposal sampler f was uniform over $[n - 1]$.

B.1.2. MODEL CONFIGURATIONS FOR GENERATIVE AIs

For each generative model, we trained two separate class-conditional models, one using the original dataset and another using the Anchor-augmented version of the dataset. The resulting Booster dataset was formed by drawing $n/2$ samples from each of the two models, sampling uniformly across classes via label conditioning. All models were trained with Adam, using $(\beta_1, \beta_2) = (0, 0.9)$ for GAN and $(\beta_1, \beta_2) = (0.9, 0.999)$ otherwise. The following summarizes the model configurations used for each model.

For **GAN**, we used a DCGAN-style architecture based on transposed convolutions. We trained the model using hinge loss. We used learning rates 10^{-4} for the generator and $2 \cdot 10^{-4}$ for the discriminator. We used batch size 128 and trained for 40 epochs on MNIST and 60 epochs on CIFAR10. The latent dimension was set to 128 for MNIST and 256 for CIFAR10.

For **DDPM**, we used a class-conditional UNet with base width 64 on MNIST and 128 on CIFAR10. We used a linear noise schedule with $\beta_{\text{start}} = 10^{-4}$ and $\beta_{\text{end}} = 0.02$, with $T = 1000$ diffusion steps. Training used learning rate 10^{-4} and batch size 64, for 30 epochs on MNIST and 200 epochs on CIFAR10. Sampling used the full DDPM sampler with 1000 steps.

For **DDIM**, we sampled from the same trained DDPM parameters, conditioning on class labels in the same manner as DDPM. We used 250 sampling steps with a linear index schedule on MNIST and an index schedule uniform in the $\bar{\alpha}$ space on CIFAR10.

For **FM**, we used the same class-conditional UNet backbone as in DDPM. Training used learning rate 10^{-4} and batch size 64, for 30 epochs on MNIST and 200 epochs on CIFAR10, using time scale 1000. Sampling solved the associated ODE using the Euler method with 50 steps on MNIST and 200 steps on CIFAR10.

We provide sample visualizations for MNIST and CIFAR10 in Figures 8 and 9, respectively.

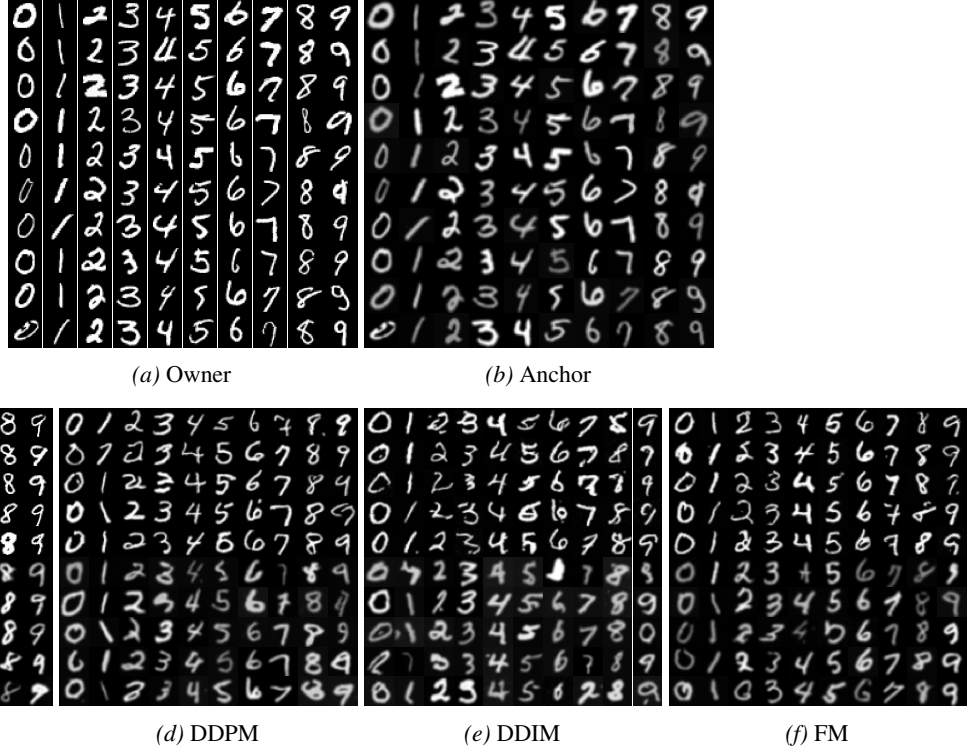


Figure 8. MNIST samples. For each generative model panel (c) to (f), the top five rows show samples generated from the model trained on the original dataset, and the bottom five rows show samples generated from the model trained on the Anchor augmented dataset.



Figure 9. CIFAR10 samples. For each generative model panel (c) to (f), the top five rows show samples generated from the model trained on the original dataset, and the bottom five rows show samples generated from the model trained on the Anchor augmented dataset.

B.1.3. ADDITIONAL RESULTS

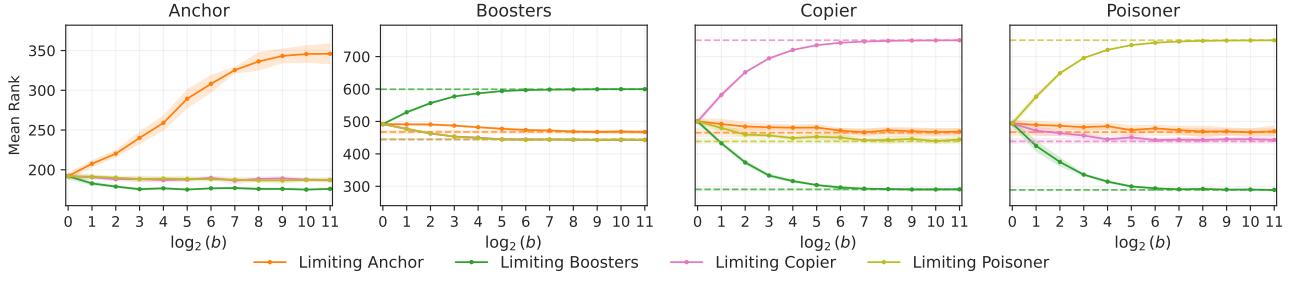


Figure 10. Change of mean rank by limiting weight of each provider.

Table 1. Provider-wise values on MNIST (mean (sd)).

Provider	SV	WSV	PSV	PASV ($b=2$)	PASV ($b=8$)	PASV ($b=32$)
Owner	0.0957 (0.0002)	0.5270 (0.0000)	0.5270 (0.0000)	0.5270 (0.0000)	0.5270 (0.0000)	0.5270 (0.0000)
Anchor	0.1148 (0.0004)	0.0468 (0.0002)	0.0927 (0.0056)	0.0826 (0.0069)	0.0673 (0.0040)	0.0548 (0.0049)
GAN	0.1225 (0.0003)	0.0596 (0.0001)	0.0483 (0.0028)	0.0513 (0.0027)	0.0512 (0.0021)	0.0562 (0.0021)
DDPM	0.1144 (0.0003)	0.0507 (0.0002)	0.0470 (0.0036)	0.0557 (0.0039)	0.0591 (0.0061)	0.0624 (0.0047)
DDIM	0.1078 (0.0003)	0.0518 (0.0002)	0.0330 (0.0034)	0.0283 (0.0045)	0.0281 (0.0079)	0.0263 (0.0032)
FM	0.1506 (0.0004)	0.0825 (0.0003)	0.0773 (0.0048)	0.0767 (0.0035)	0.0884 (0.0054)	0.0960 (0.0070)
Copier	0.0848 (0.0003)	0.0073 (0.0002)	-0.0032 (0.0022)	-0.0065 (0.0012)	-0.0054 (0.0005)	-0.0061 (0.0006)
Poisoner	0.0175 (0.0003)	-0.0178 (0.0002)	-0.0141 (0.0052)	-0.0072 (0.0015)	-0.0077 (0.0009)	-0.0086 (0.0012)

Priority-Aware Shapley Value

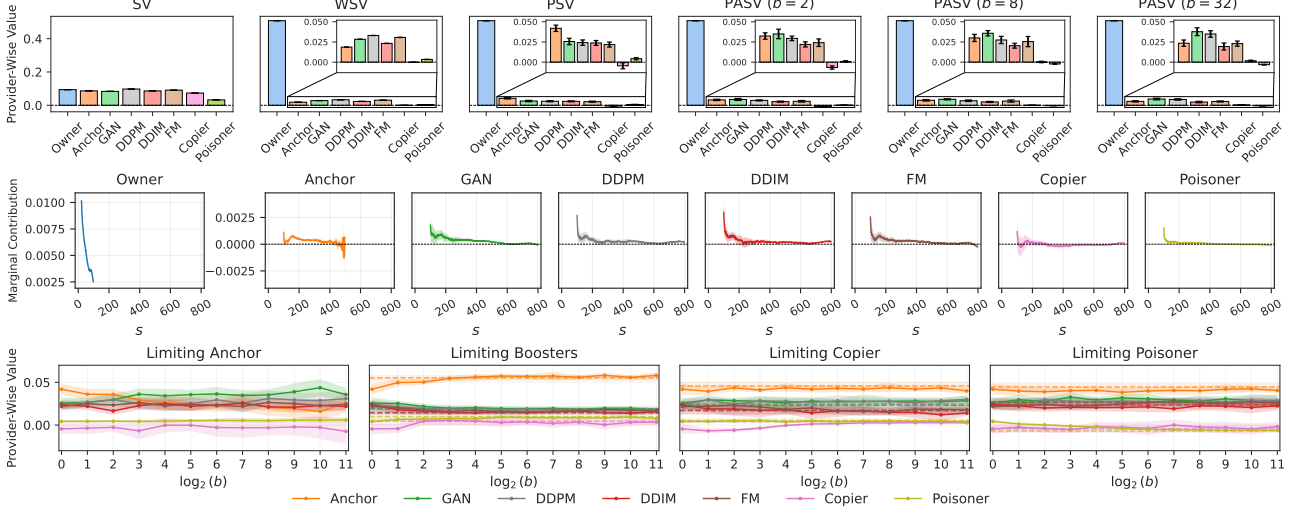


Figure 11. CIFAR10 results. **(Top)** Provider-wise values. **(Middle)** Marginal contribution versus subset size. **(Bottom)** Sensitivity analysis.

Table 2. Provider-wise values on CIFAR10 (mean (sd)).

Provider	SV	WSV	PSV	PASV ($b=2$)	PASV ($b=8$)	PASV ($b=32$)
Owner	0.0939 (0.0003)	0.5080 (0.0000)	0.5080 (0.0000)	0.5080 (0.0000)	0.5080 (0.0000)	0.5080 (0.0000)
Anchor	0.0866 (0.0003)	0.0186 (0.0001)	0.0419 (0.0039)	0.0324 (0.0040)	0.0300 (0.0045)	0.0235 (0.0040)
GAN	0.0835 (0.0002)	0.0283 (0.0001)	0.0256 (0.0040)	0.0349 (0.0059)	0.0358 (0.0033)	0.0377 (0.0049)
DDPM	0.0977 (0.0004)	0.0330 (0.0001)	0.0242 (0.0034)	0.0294 (0.0029)	0.0274 (0.0045)	0.0349 (0.0041)
DDIM	0.0864 (0.0003)	0.0232 (0.0001)	0.0238 (0.0030)	0.0220 (0.0032)	0.0204 (0.0030)	0.0194 (0.0044)
FM	0.0910 (0.0003)	0.0306 (0.0001)	0.0218 (0.0031)	0.0241 (0.0047)	0.0255 (0.0063)	0.0229 (0.0032)
Copier	0.0736 (0.0004)	-0.0002 (0.0001)	-0.0045 (0.0037)	-0.0066 (0.0020)	0.0002 (0.0009)	0.0017 (0.0007)
Poisoner	0.0324 (0.0002)	0.0034 (0.0001)	0.0043 (0.0014)	0.0009 (0.0010)	-0.0022 (0.0004)	-0.0031 (0.0005)

Algorithm 2 Utility evaluation with conditional k NN imputation.

Input: training set $\mathcal{D}_{\text{train}} = \{(x'_i, y'_i)\}_{i=1}^{n_{\text{train}}}$; test set $\mathcal{D}_{\text{test}} = \{(x_i, y_i)\}_{i=1}^{n_{\text{test}}}$; trained predictor f ; subset $S \subseteq [n]$; number of neighbors k ; number of evaluation points n_{eval} .

Initialize $\widehat{U}(S) \leftarrow 0$

for $t = 1$ **to** n_{eval} **do**

- Sample (x, y) uniformly from $\mathcal{D}_{\text{test}}$
- Find k nearest neighbors $\{x^{(1)}, \dots, x^{(k)}\}$ of x among $\{x'_i\}_{i=1}^{n_{\text{train}}}$ restricted to coordinates in S
- Initialize** $\widehat{u} \leftarrow 0$
- for** $j = 1$ **to** k **do**

 - Form composite input $\tilde{x}^{(j)} \leftarrow x_S \oplus x_{S^c}^{(j)}$
 - $\widehat{u} \leftarrow \widehat{u} + f_y(\tilde{x}^{(j)})$

- end for**
- $\widehat{U}(S) \leftarrow \widehat{U}(S) + \widehat{u}/k$

end for

$\widehat{U}(S) \leftarrow \widehat{U}(S)/n_{\text{eval}}$

return $\widehat{U}(S)$

B.2. Experiment in Section 5.2

B.2.1. ON-MANIFOLD UTILITY WITH CONDITIONAL k -NN IMPUTATION

Feature attribution evaluates how a fixed trained predictor changes as features are revealed, so we define the utility of a feature subset through a masking-based prediction score. Let $f_y(x)$ denote the predicted probability assigned to class y at input x .

For a subset of feature indices $S \subseteq [n]$ and a labeled test point (x, y) , the utility is computed by keeping the observed coordinates x_S fixed and imputing the remaining coordinates x_{S^c} from a conditional reference distribution rather than from the marginal (Janzing et al., 2020; Sundararajan & Najmi, 2020; Frye et al., 2021). This on-manifold construction is used to avoid implausible masked inputs that can arise under marginal imputation when features are dependent.

Concretely, we approximate the conditional distribution of the unobserved coordinates given the observed ones, $p(x_{S^c}|x_S)$, using k -NN sampling in the subspace restricted to coordinates in S . Given a test point (x, y) and S , let $\{x^{(1)}, \dots, x^{(k)}\}$ denote the k nearest neighbors of x among training inputs when distances are computed using only the coordinates in S . For each neighbor $x^{(j)}$, we form a composite input $x_S \oplus x_{S^c}^{(j)}$, which keeps the coordinates in S from x and fills the remaining coordinates from $x^{(j)}$. The per-point utility is defined as the conditional expectation

$$u_S(x, y) = \mathbb{E}_{x'_{S^c} \sim p(x'_{S^c}|x_S)} [f_y(x_S \oplus x'_{S^c})],$$

and is estimated using the k -NN conditional sampler by

$$\widehat{u}_S(x, y) = \frac{1}{k} \sum_{j=1}^k f_y(x_S \oplus x_{S^c}^{(j)}).$$

Finally, following the global aggregation used in Shapley-based feature attribution, we define the subset utility as

$$U(S) = \mathbb{E}_{(x, y) \sim p(x, y)} [u_S(x, y)].$$

In implementation, we estimate $U(S)$ by Monte Carlo using n_{eval} test points $(x^{(t)}, y^{(t)})$ sampled uniformly from the test split and the k -NN estimator $\widehat{u}_S(x, y)$, i.e.,

$$\widehat{U}(S) = \frac{1}{n_{\text{eval}}} \sum_{t=1}^{n_{\text{eval}}} \widehat{u}_S(x^{(t)}, y^{(t)}).$$

Implementation details of the utility evaluation procedure are provided in Algorithm 2.

B.2.2. DETAILED SETUP

We provide further implementation details for the feature attribution experiments in Section 5.2. We used a fixed random seed for the train test split, and replicated value estimation across 10 independent random seeds. In the results, we report the mean and one standard deviation across these runs.

The experimental setup largely followed Frye et al. (2020). The Census Income dataset was preprocessed by dropping samples with missing values, yielding 45,222 samples with 12 features (intentionally excluding fnlwgt and education-num), followed by a 75/25 train test split. All categorical features were encoded using one hot encoding, while continuous features were standardized to have zero mean and unit variance. An MLP classifier f was trained with ReLU activations and ℓ_2 regularization with coefficient 10^{-4} . Optimization used Adam with $(\beta_1, \beta_2) = (0.9, 0.999)$ and learning rate 10^{-3} . Training ran for up to 200 epochs with batch size 128, using early stopping with a validation fraction of 0.25 and a patience of 20 epochs. For the conditional sampler used to evaluate $U(S)$, we set $k = 100$, $n_{\text{eval}} = 1000$ and used Euclidean distance. All values were estimated based on $N_{\text{MC}} = 3000$ Monte-Carlo samples, and for the general DAG setting, linear extensions were sampled using Algorithm 1 with burn-in $B = 10,000$ and thinning $\tau = 1,000$.

B.2.3. DAG CONSTRUCTION FOR CENSUS INCOME DATASET VIA LLM CONSULTATION

In this experiment, the detailed precedence DAG over the 12 Census Income features was obtained by starting from the coarse ordered-partition constraint of Frye et al. (2020) and consulting **ChatGPT 5.2 Thinking** only to propose candidate relations based on common sense and domain knowledge. Note that we are not making a causal claim providing this DAG, and the full conversation transcript is provided below for transparency.

Prompt

We consider the U.S. Census Income dataset for predicting whether annual income exceeds \$50K. Features included in the dataset are as below:

- age: age in years.
- workclass: employment type (e.g., Private, Self-emp, Gov).
- education: highest education level attained (categorical; e.g., Bachelors, HS-grad, etc.).
- marital-status: marital status (e.g., Married-civ-spouse, Never-married, Divorced, etc.).
- occupation: job category (e.g., Tech-support, Craft-repair, Exec-managerial, etc.).
- relationship: household relationship/role (e.g., Husband, Wife, Own-child, Not-in-family, etc.).
- race: self-identified race category.
- sex: biological sex / gender as recorded (Male/Female).
- capital-gain: capital gains (numeric).
- capital-loss: capital losses (numeric).
- hours-per-week: usual hours worked per week (numeric).
- native-country: country of origin (categorical).

We treat each input variable as a player in a cooperative game and use a DAG over features to encode precedence constraints for feature attribution. For constructing a DAG, a common approach in existing papers is to partition variables into two blocks: A (demographic): {age, race, sex, native-country} B (socioeconomic): {workclass, education, marital-status, occupation, relationship, capital-gain, capital-loss, hours-per-week} and assume a complete bipartite DAG $A \rightarrow B$ (i.e., every variable in A has a directed edge into every variable in B), with no edges within A and no edges within B.

Please evaluate whether the DAG specified above is reasonable. If it is, simply say: "The specified DAG is reasonable." and ignore everything below. If it is not, propose a more realistic DAG that better reflects plausible relationships among these variables.

If you propose a new DAG, first provide a brief paragraph explaining your design principles for the DAG, and then provide the DAG as an edge list in the form (parent \rightarrow child).

Response

The specified bipartite DAG $A \rightarrow B$ is not very realistic. While it's sensible that demographic variables often precede many socioeconomic outcomes, the assumption of no edges within B is a major miss: there are strong, plausible precedence relations like education \rightarrow occupation/workclass, marital-status \rightarrow relationship, and occupation/workclass \rightarrow hours-per-week, etc. Treating all B variables as mutually "parallel" can distort attributions by forcing effects that plausibly flow through education/occupation to instead be credited directly to demographics.

Design principles

I'm aiming for a DAG that (1) respects temporal/structural precedence (stable attributes and early-life factors precede later labor-market outcomes), (2) captures the most obvious within-socioeconomic dependencies (especially education \rightarrow occupation/workclass and marital-status \rightarrow relationship), (3) stays sparse and defensible (only edges that are broadly plausible across the population), and (4) avoids dubious causal claims (e.g., race \leftrightarrow native-country) by not forcing edges where directionality is unclear.

Proposed DAG (edge list)

```
(age -> education)
(age -> marital-status)
(age -> occupation)
(age -> relationship)
(age -> capital-gain)
(age -> capital-loss)
(sex -> education)
(sex -> occupation)
(sex -> workclass)
(sex -> marital-status)
(sex -> relationship)
(race -> education)
(race -> occupation)
(race -> workclass)
(native-country -> education)
(native-country -> occupation)
(native-country -> workclass)
(education -> occupation)
(occupation -> workclass)
(occupation -> hours-per-week)
(workclass -> hours-per-week)
(education -> capital-gain)
(education -> capital-loss)
(occupation -> capital-gain)
(occupation -> capital-loss)
(marital-status -> relationship)
```

This keeps the intuitive "demographics often precede socioeconomic outcomes" idea, but also encodes key intra- B precedence constraints that the complete bipartite $A \rightarrow B$ structure cannot represent.

Table 3. Average marginal contribution of capital-gain under different ordering with marital-status and capital-loss; The baseline sampling distribution ($\lambda = 1$) is used. Entries report mean (sd) across replications.

Case of Ordering	Proportion in Samples	Marginal Contribution
marital-status \rightarrow capital-gain \rightarrow capital-loss	0.3873 (0.0087)	0.01663 (0.00000)
{marital-status, capital-loss} \rightarrow capital-gain	0.4620 (0.0087)	0.01807 (0.00001)
capital-gain \rightarrow {marital-status, capital-loss}	0.1134 (0.0062)	0.01835 (0.00002)
capital-loss \rightarrow capital-gain \rightarrow marital-status	0.0373 (0.0048)	0.02040 (0.00004)

B.2.4. ADDITIONAL RESULTS

Sweep Diagnostics. As shown in Figure 12 (and in the right panel of Figure 7), we notice that varying the priority weights to promote or delay a given feature does not necessarily induce a monotone change in its estimated value. Motivated by these non-monotone responses, we conduct a diagnostic analysis and focus on a representative case that exhibits a obvious U-shaped pattern under the sweep, capital-gain. First, based on the general DAG in Figure 6b, we can anticipate what happens in each limiting case. Clearly, since capital-gain is maximal in the full player set, in the $\lambda \rightarrow \infty$ scenario it is placed at the very end of the linear extension with probability one. On the other hand, in the $\lambda \rightarrow 0^+$ case, capital-gain is promoted as much as possible until it becomes the unique element of the maximal set. In particular, in the perspective of the backward sampling scheme, {age, sex, native-country, race, education, occupation} (and only these) always appear before it, so under the limiting distribution capital-gain occupies seventh position with probability one (which is also consistent with the rank pattern in Figure 13). Meanwhile, we observed the following interesting relationship among the three players capital-gain, capital-loss, and marital-status:

1. capital-gain attains a **larger** marginal contribution when capital-loss has already been included in the model.
2. capital-gain attains a **smaller** marginal contribution when marital-status has already been included in the model.

To support this, Table 3 partitions sampled linear extensions by the relative ordering among capital-gain, capital-loss, and marital-status, and reports the corresponding mean marginal contribution of capital-gain. The table shows a dependence among three features. When marital-status precedes capital-gain while capital-loss remains absent, the marginal contribution of capital-gain is the smallest, and this happens frequently. In contrast, when capital-loss precedes capital-gain and marital-status is still absent, capital-gain achieves the largest marginal contribution, although it occurs rarely. The mixed case, where capital-gain appears after both marital-status and capital-loss (as in $\lambda \rightarrow \infty$) or before both (as in $\lambda \rightarrow 0^+$) yield intermediate marginal contributions. Noting that the weight average of the marginal contribution in Table 3 is a value of capital-gain under $\lambda = 1$, this clarifies the U-shape behavior of the sweeping result. In summary, capital-loss acts as an amplifying context for capital-gain, whereas marital-status acts as a suppressing context, and the priority sweep modulates the value of capital-gain value primarily through shifting the frequencies of these contexts.

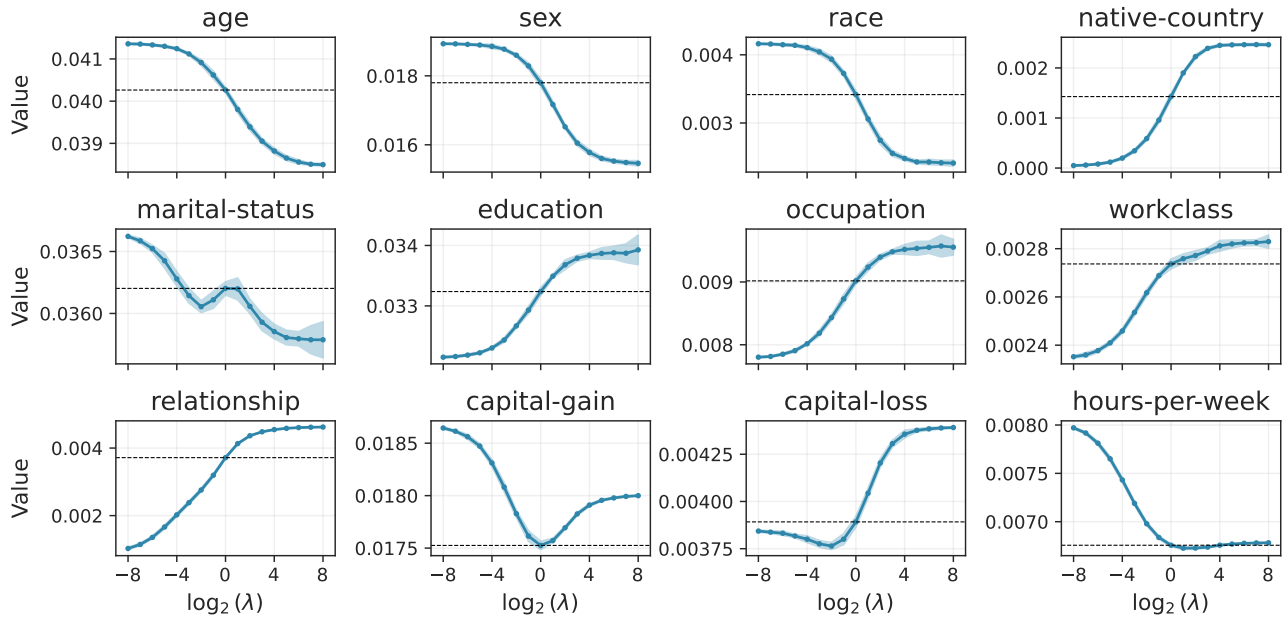


Figure 12. Change of feature value from priority sweep on the Census Income dataset.

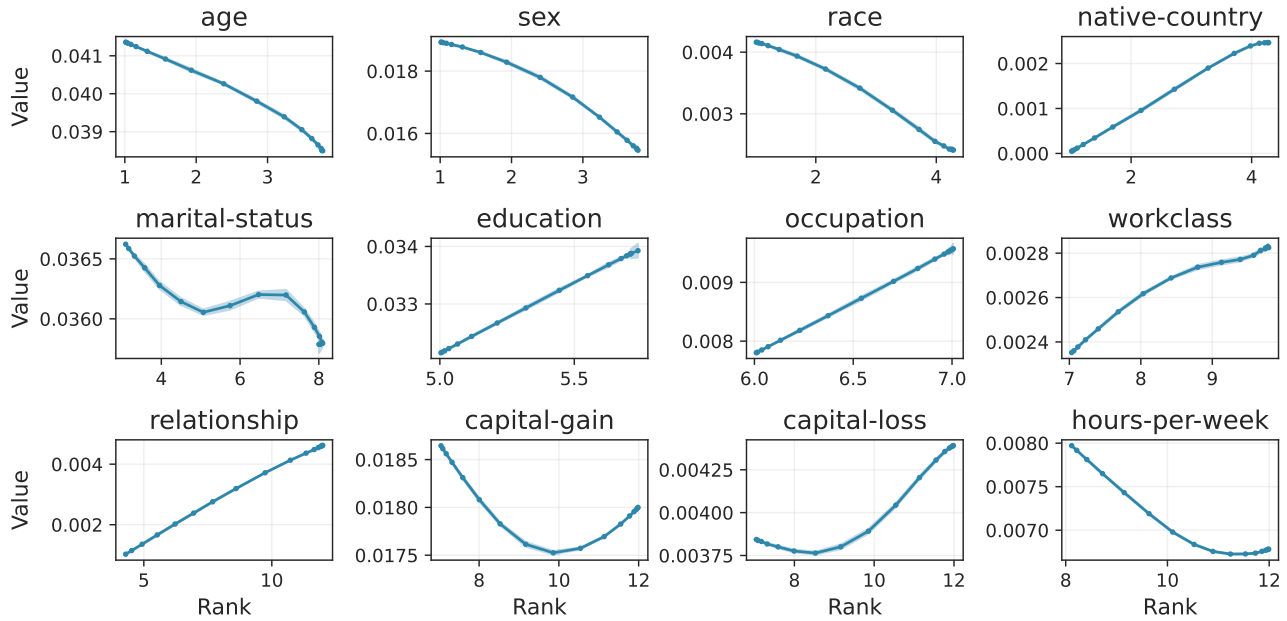


Figure 13. Feature values as a function of the feature's rank induced by priority sweep.